INSTITUT DE FRANCE
Académie des sciences

Comptes Rendus

Mécanique

Laikuang Lin, Yimin Xia, Xuhui Zhang, Liang Yi and Jie Fu

Comparison study on rock breaking characteristics of disc cutters under coupled static–dynamic loads and static loads

Volume 351 (2023), p. 1-15

Published online: 12 January 2023

https://doi.org/10.5802/crmeca.163

CENTRE MERSENNE

Les Comptes Rendus. Mécanique *sont membres du Centre Mersenne pour l'édition scientifique ouverte*
www.centre-mersenne.org
e-ISSN : 1873-7234

Comptes Rendus
Mécanique
2023, Vol. 351, p. 1-15
https://doi.org/10.5802/crmeca.163

Synthesis / *Synthèse*

Comparison study on rock breaking characteristics of disc cutters under coupled static–dynamic loads and static loads

Laikuang Lin [*, a], Yimin Xia [a], Xuhui Zhang [a], Liang Yi [a] and Jie Fu [*, b]

[a] College of Mechanical and Electrical Engineering, State Key Laboratory of High Performance Complex Manufacturing, Central South University, Changsha 410083, China

[b] School of Materials Science and Engineering, Central South University, Changsha 410083, China

E-mails: linlaikuang@csu.edu.cn (L. Lin), xiaymj@csu.edu.cn (Y. Xia), 153701027@csu.edu.cn (X. Zhang), 562898830@qq.com (L. Yi), fj1221@csu.edu.cn (J. Fu)

Abstract. Rock cutting methods for disc cutters with coupled static–dynamic loads and static loads are explored and compared through rock breaking experiments to improve the TBM excavation efficiency. Results indicate that the rock breaking characteristics, including rock debris, cutting force, and rock breaking efficiency, significantly varies with different cutting methods. The average size of rock fragmentation produced under coupled static–dynamic loads is 1.6 times larger than that under static loads. The cutting forces of disc cutter under the coupled static–dynamic loads are larger than those under static loads when the cutting depth (h) is lower than 4 mm, whereas is contrary when h exceeds 4 mm. The specific energy of disc cutter under the coupled static–dynamic load is approximately 1.5 times smaller than that under the static load, indicating the cutting method with the coupled static–dynamic load can significantly improve the cutting performance. There is an optimal cutter spacing (S) for the cutter under each cutting method. The optimal S under the coupled static–dynamic loads is larger than that with static loads. This study provides new insights into improving the tunneling efficiency in high-strength rock conditions.

Keywords. TBM, Disc cutter, Coupled static–dynamic loads, Rock breaking efficiency, Cutting force.

Manuscript received 8 September 2020, revised 19 December 2022, accepted 20 December 2022.

1. Introduction

Tunnel boring machines (TBMs) are widely applied in tunnel excavation due to their high excavation efficiency, high construction quality, and low ground disturbance [1, 2]. Disc cutters installed on the TBM cutterhead are the main rock breaking tools that interact with and cut rock directly through the rotation of the cutterhead during the TBM tunneling process [3].

* Corresponding authors.

The comprehensive performance of TBMs is mainly influenced by the rock breaking characteristics of cutter. Therefore, many researchers have investigated the rock breaking process of disc cutters through experiments, simulations, and engineering analysis.

In the aspect of rock breaking experiment, Rostami [4] and Gertsch *et al.* [5] conducted large-scale rock breaking experiments by using the linear cutting machine (LCM) and developed the CSM (Colorado School of Mines) cutting force prediction model of disc cutters. Cardu *et al.* [6] designed a novel LCM and used it to reveal the rock breaking characteristics of disc cutters interacting with different types of rocks. Liu *et al.* [7,8] studied the influence of confining stresses on rock breaking characteristics, and revealed the coupled influence of surface and internal crack propagation on rock breakages. Lin *et al.* [9] revealed the crack propagation and failure modes induced by the disc cutter when the confining stresses and joint characteristics vary through a series of rock breaking tests. Some scholars have studied the rock breaking characteristics of disc cutter through simulation or simulation combined with experiment. Geng *et al.* [10] compared the rock breaking characteristics of gauge and normal cutters through cutting tests and simulations. Cho *et al.* [11, 12] obtained the optimal parameters of cutting depth and spacing for disc cutters on the basis of the cutter cutting efficiency through simulation and rock breaking test. Labra *et al.* [13] used the hybrid discrete/finite element model to study the cutting mechanism of the TBM disc cutter, and the simulation results are consistent with both experiments and theoretical predictions. Bejari *et al.* [14] investigated the influences of rock joint space and orientation on rock fragmentation induced by TBM disc cutter using the discrete element numerical method. Naghadehi and Mikaeil [15] simulated the evolution law of cracks produced by cutters and determined the optimal cutting condition. Zhang *et al.* [16] investigated the rock fragmentation induced by wedge cutter in mixed ground by using experiments and simulation and proposed that the penetration rate should be slowed down to prevent cutter damage. Zhai *et al.* [17] and Zhou *et al.* [18] investigated the rock fragmentation by TBM cutters through a novel numerical method called general particle dynamics.

The aforementioned studies provide a thorough background of the rock breaking process for TBM disc cutters and present a good reference for cutter layout and cutterhead design. However, along with the development of tunnel engineering in recent years, TBM has faced a series of problems during the tunneling process, especially the engineering issues related to tunneling efficiency and construction cost of TBM under complex and harsh geological conditions. Considering a Chinese water diversion tunnel project as an example, the rock encountered by the TBM in this project exhibited the features of high strength, large buried depth, and high quartz content. Due to the harsh geological conditions, the penetration rate of disc cutter was below 2 mm/rev, the average normal thrust for each cutter reached 300 kN, and the TBM tunneling distance was less than 4 km in nearly two years, resulting in a low tunneling efficiency and high engineering cost.

As mentioned above, the TBM excavation efficiency is mainly determined by the rock breaking efficiency of disc cutters. Therefore, several novel rock breaking methods for TBMs have been developed and applied to improve the TBM tunneling efficiency and control the construction cost under the complex harsh geological conditions. For instance, Ciccu and Grosso [19] introduced the cutting characteristics of disc cutters assisted with a high-pressure water jet. Liu *et al.* [20] investigated the cutting performance of cutting head for rock cutting assisted with multi-water jets and found that the high-pressure water jet benefits the rock breaking ability. Hassani *et al.* [21] proposed a new rock cutting approach that employed microwave irradiation. Geng *et al.* [22] proposed a novel rock breaking method, called a free-face-assisted method, and designed a multistage cutterhead for TBM. For rock properties and cutter layout, the aforementioned rock breaking methods have been proposed, and proper attempts have been made. However, the proposed methods have not yet completely solved the problem of low excavation efficiency

Figure 1. Linear cutting machine.

for TBM. Therefore, innovative rock breaking methods with better rock breaking efficiency are still required.

Based on the rock breaking mechanisms and loading conditions, rock breaking cutting tools can be divided into those that work under static loads, dynamic/impact loads, and coupled static–dynamic loads. Li *et al.* [23–25] introduced and developed the coupled static and dynamic loading theory and applied it to mining engineering. They observed that compared with the static load mode, choosing a reasonable combination of static and dynamic loads significantly improves the energy utilization rate of tools and rock breaking efficiency.

There are two rock cutting modes, constant penetration and constant thrust mode for conventional TBM, both of which are attributed to the rock breaking method under static loads, i.e., the conventional rock breaking method of the disc cutter is rolling rock-breaking under static loads [26]. To improve the rock breaking efficiency of disc cutters, it could be an effective and achievable attempt to transform the cutter rock breaking method into the coupled static–dynamic loading mode. Therefore, a novel rock breaking method of disc cutter under coupled static–dynamic loads is proposed in this paper. Further, the differences in rock breaking characteristics between the coupled static–dynamic and conventional static loading methods are investigated on the basis of rock breaking experiments conducted in this study.

2. Test methodology

2.1. *Test bench*

The self-designed LCM located at Central South University for testing rock breaking is shown in Figure 1, and it consists primarily of hydraulic, cutting, and testing systems. The dimension of the entire test bench is $5000 \times 3200 \times 3500$ mm^3. The main components include a console, hydraulic workstation, longitudinal cylinder, lateral cylinder, vertical cylinder, impact dynamic oil cylinder, rock bin, movable beam, and frame.

In the cutting system, cutting tools and the three-direction force sensor are mounted on the tool carriers. Different kinds/sizes of cutting tools can be mounted for each cutting test by changing the type and structure of the cutter carriers. Cutting forces, including normal force,

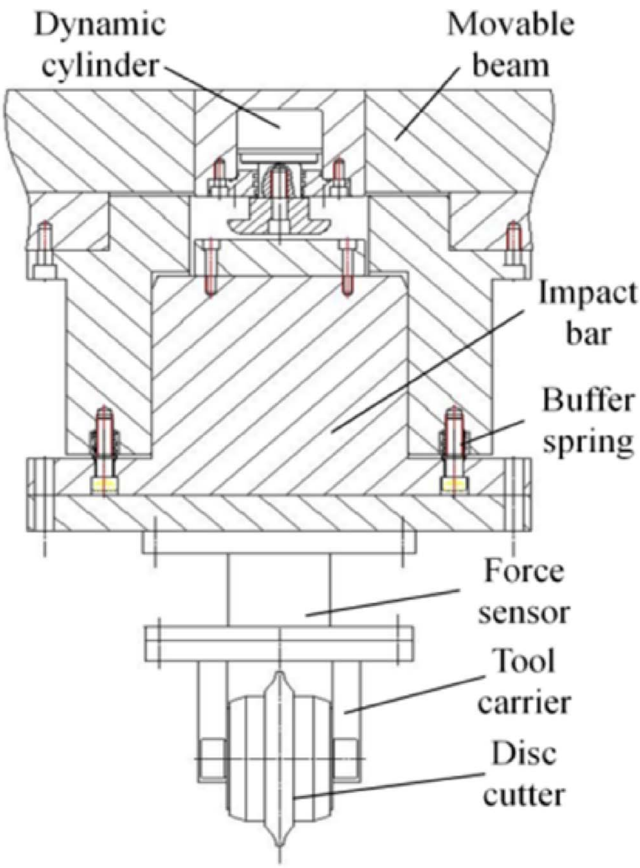

Figure 2. Device structure used to apply coupled static–dynamic loads.

rolling force, and side force, are measured by the three-direction force sensor and recorded by the testing system. The testing system consists of a computer, data acquisition card, voltage-stabilized source, and National Instruments LabVIEW.

The device structure used to apply coupled static–dynamic loads is shown in Figure 2. The static loads are applied to the disc cutter by setting a constant cutting depth, which can be controlled by the vertical hydraulic cylinder and locking device. The displacement sensor monitors the cutting depth. The interval dynamic loads are realized by the dynamic oil cylinder and are transferred to the disc cutter through the tool carriers. The lateral cylinder is responsible for the lateral feed of the rock bin to adjust the cutter space, whereas the longitudinal cylinder is applied for the longitudinal movement of the rock bin to achieve straight cutting. The limit of the working pressure of the hydraulic cylinder is 20 MPa.

2.2. *Cutter and rock specimen*

The cutting tool employed in the rock breaking tests was a laboratory-scale constant cross-section (CCS) type disc cutter with diameter and cutter blade width of 216 mm and 9.5 mm, respectively; it is half the size of an actual cutter, as shown in Figure 3.

Marbles were selected as the rock samples and were sufficiently large (nominally 900 × 380 × 260 mm^3) so that edge effects were avoided, and cutting tests could be repeated for a sufficient

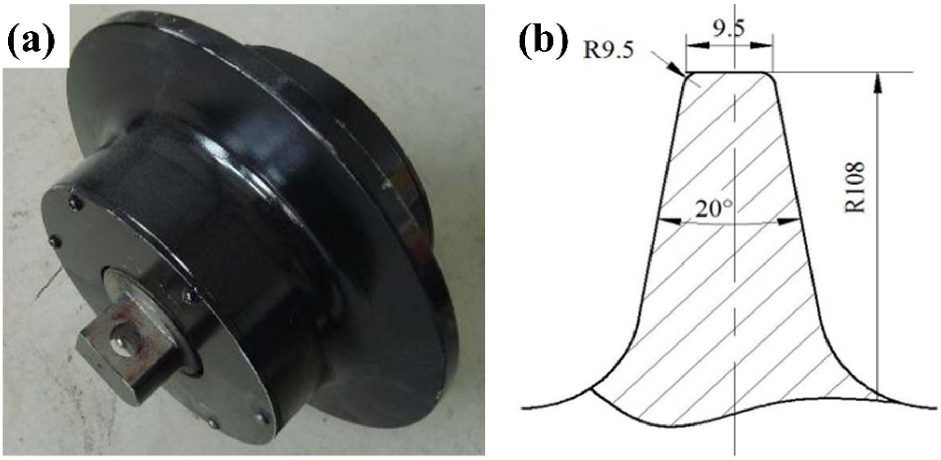

Figure 3. Structure of disc cutter: (a) Disc cutter; (b) structural size of cutter blade.

Table 1. Properties of rock samples used in tests

Density ($kg \cdot m^{-3}$)	Young modulus (GPa)	Uniaxial compressive strength (MPa)	Brazilian tensile strength (MPa)	Poisson's ratio
2580.0	7.1	26.3	5.2	0.2

Table 2. Cutting parameter setting

Cutting parameters	Values
h (mm)	2, 3, 4, 6
S (mm)	30, 40, 60, 80

amount of time. The rock sample was cast in concrete in an open-bottomed steel rock bin, which could be mounted onto the table of the LCM. The properties of the rock sample are listed in Table 1. Several cuts were made on each sample before the data acquisition began to ensure that the rock surface was fully conditioned.

2.3. *Test procedures*

Two cutting modes, coupled static–dynamic loads and static loads, were applied. To test the cutting mode under the static loads, the disc cutter is controlled to move up and down to achieve the specified cutting depth by the vertical hydraulic cylinder and then driven by a constant cutting speed to cut the rock via the longitudinal cylinder. To test the cutting mode under the coupled static–dynamic loads, based on cutting mode with the static loads, the dynamic load is applied to the disc cutter through a dynamic oil cylinder, as shown in Figure 4. In this study, the pressure of the hydraulic cylinder for the impact loading is set to 20 MPa, and the impact load is approximately 5 kN. The dynamic velocity of the disc cutter is 2.5 m/s, and the loading frequency is 1 Hz.

The feed speed is set to 20 mm/s, and the cutting distance is 400 mm. According to TBM engineering data, the cutter spacings of an actual TBM are usually set to 50 to 90 mm, whereas the cutting depths are controlled within 10 mm. Thus, the parameters of cutting depth (h) and cutter spacing (S) employed in the tests are determined and listed in Table 2. When S is studied, h is set to 4 mm; when h is studied, S is set to 40 mm.

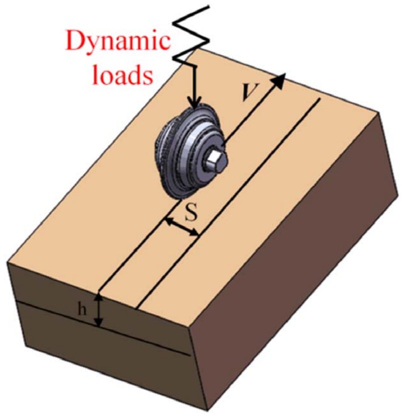

Figure 4. Schematic diagram of cutting mode under coupled static–dynamic loads.

3. Results

3.1. *Rock Debris*

The rock breaking characteristics for the two different kinds of cutting modes are depicted in Figure 5 when h and S are 4 mm and 60 mm, respectively. The rock debris produced on both sides of the cutter tip is similar to slag powder when cutting rock under static loads, as illustrated in Figure 5a. When breaking rock with the coupled static–dynamic loads, a large amount of big rock debris can be observed on both sides of the cutter tip, and the maximum size of rock debris is larger than 68 mm, as shown in Figure 5b. The collected rock debris under different modes is depicted in Figure 6. The size and volume of rock debris produced under static loads are much smaller than those under the static–dynamic loads with the same h. It can be concluded that the cutting method under the coupled static–dynamic loads can significantly improve the cutter rock-breaking performance with such cutting parameters.

Square hole sieves of five sizes were used to sieve the rock debris under different cutting test: 53 mm, 37.5 mm, 9.5 mm, 2.36 mm, and 0.6 mm, according to the national standard (100 mm as the reference sieve pore and $\sqrt[10]{10} = 1.259$ as the differential). The average fragmentation size was calculated based on the measured average size of the crushed rock block for each pore size, and the percentage of the rock debris mass corresponding to the total crushed block mass. Figure 7 shows the relationship between the average fragmentation size and h. For the two cutting modes, the average fragment size increases along with the increase of h. However, the increasing velocity slows down when h reaches 4 mm. With the same h, the average fragment size produced under the coupled static–dynamic loads is larger than that with static loads and the average fragment size of the former is approximately 1.6 times that of the latter.

The relationship between the average fragmentation size and S is shown in Figure 8. For the two cutting modes, the average fragmentation size increases at first and subsequently declines with the increase in cutter spacing. The largest values of the average fragment size are obtained when S is 60 mm, which are 11.75 mm and 18.91 mm, respectively, for static and coupled static–dynamic loads. When S is the same, the average fragment produced under the coupled static–dynamic loads is larger than that produced under the static loads on the whole. According to the experimental phenomenon, when S is 20 mm or 40 mm, it causes certain damage to the rock mass after the preceding cutting induced by the previous cutter, which causes excessive breakage

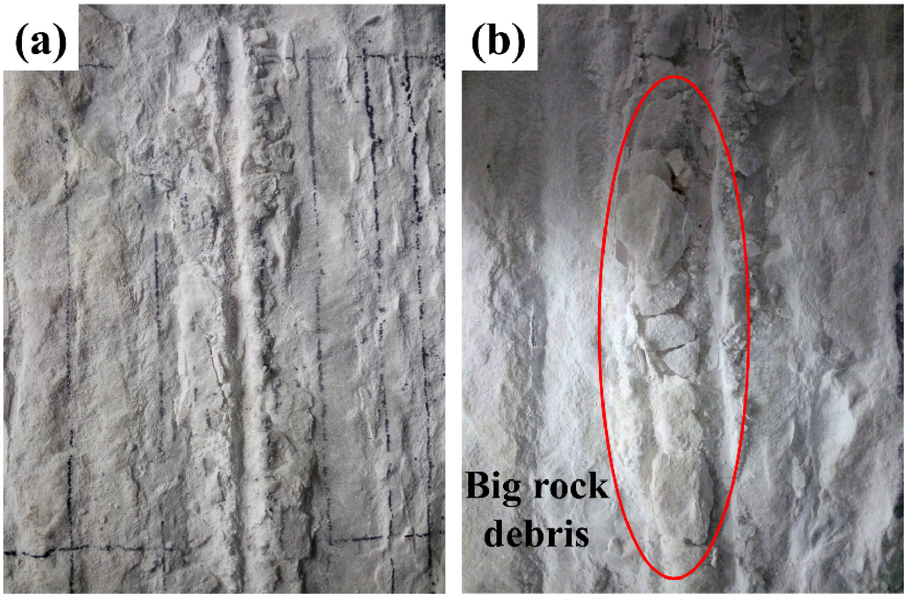

Figure 5. Rock breaking characteristics under two cutting modes: (a) under static loads; (b) under coupled static–dynamic loads.

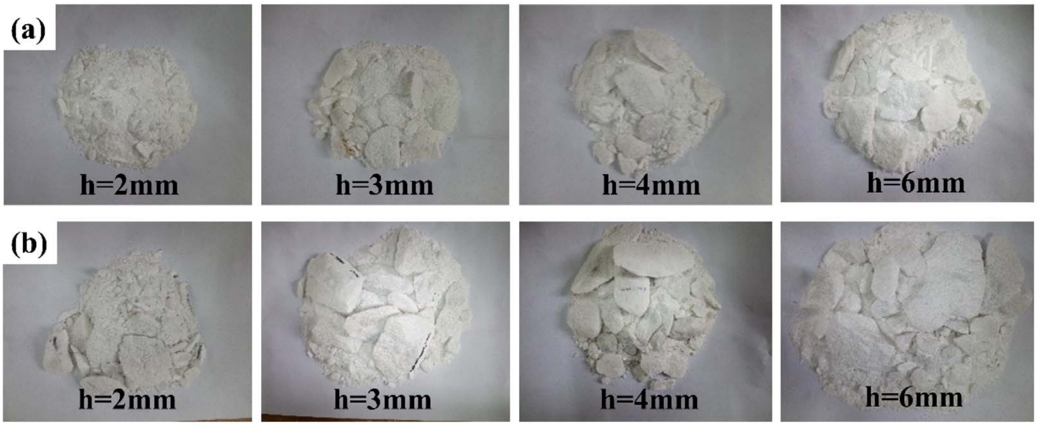

Figure 6. Rock debris under two cutting modes: (a) under static loads; (b) under coupled static–dynamic loads.

of the surface ridge between cutting grooves. However, when the cutter spacing is set to 60 mm, the surface ridge between the rock grooves is broken off, more complete rock debris is formed, and the peeling depth of the rock ridge under the coupled static–dynamic loads is larger than that with static loads. It also indicates that cutting rock under coupled static–dynamic loads is more conducive to crack propagation and the formation of bigger rock debris. When the cutter spacing is increased to 80 mm, the surface ridge cannot be peeled off under these two kinds of modes, leading to a decrease in rock debris size.

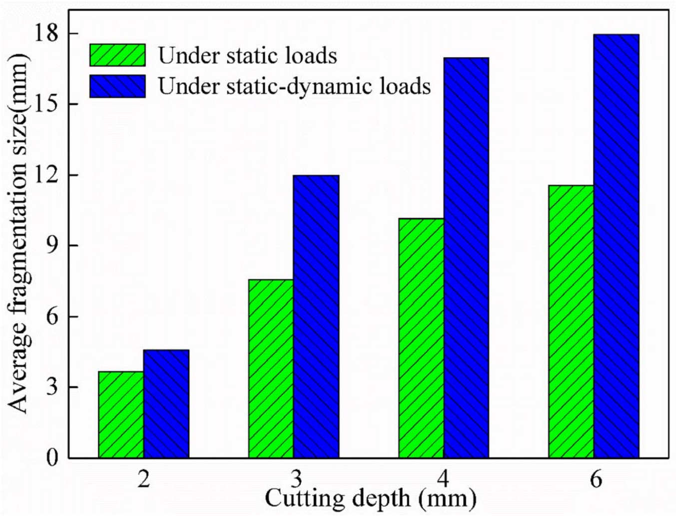

Figure 7. Relationship between average fragmentation size and h.

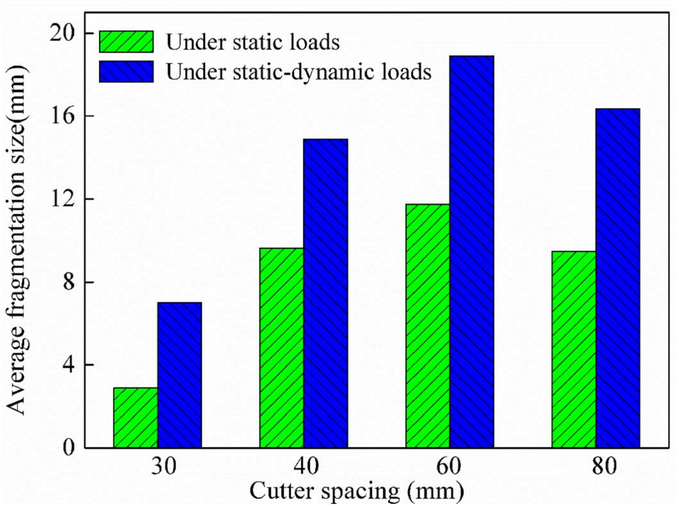

Figure 8. Relationship between average fragmentation size and S.

3.2. *Cutting force*

The cutter suffers from three-directional cutting forces, namely normal, rolling, and side forces. In this study, only the normal force and rolling force are studied, as the side force is quite small. The average cutting forces under the two kinds of cutting modes are shown in Figure 9. The normal force is greater than the rolling force for both kinds of cutting modes. When cutting rock under the static loads, the normal force and rolling force both increase with the increase in h and the increasing velocity slows down when h is increased to 4 mm. For the coupled static–dynamic loads mode, when h is lower than 4 mm, the cutting force increases significantly with the increase in h. When h is beyond 4 mm, the cutting force decreases with the increase in h. Comparing the two kinds of cutting mode, when h is lower than 4 mm, the cutting forces under coupled

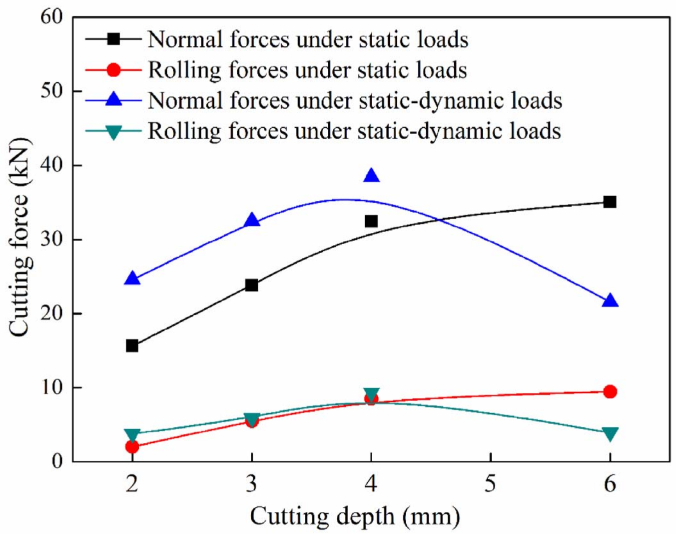

Figure 9. Relationship between cutting force and h.

static–dynamic loads are larger than those under static loads. The normal force under static–dynamic loads with the cutting depth of 2 mm is 24.57 kN whereas that under static loads in only 15.63 kN. However, when h is beyond 4 mm, the cutting forces under coupled static–dynamic loads are smaller than those under static loads. The value of normal force under static–dynamic loads changes to 21.59 kN with a depth of 6 mm, whereas that under static loads increases to 35.04 kN with the same cutting depth. It can be explained that it will cause greater damage to the rock mass after the preceding cutting induced by the disc cutter since h reaches to a larger value, especially in the case of the coupled static–dynamic loads, resulting in a sharp decline in the cutting force.

The relationship between the average cutting forces and S is shown in Figure 10. The cutting forces for both kinds of cutting modes increase significantly with the increase in S and the cutting forces under the coupled static–dynamic loads are greater than those under the static loads. Moreover, the difference in normal force for the two kinds of cutting modes is greater than that of rolling force. The difference in normal force for both kinds of cutting modes increases with the increase in S and reaches the maximum value of 11.4 kN when S is 80 mm (the value is 4.35 kN when the cutter spacing is 30 mm). This is mainly because the mutual interference between the cutting grooves is relatively large when S is small. Thus, the value of normal force remains small when disc cutter cuts rock under the coupled static–dynamic loads. However, when S is relatively large, there is no evident interaction between the cutting grooves, and the normal force will increase significantly when cutting rock under the coupled static–dynamic loads, leading to an increase in the difference of normal force between the two kinds of cutting modes.

3.3. *Cutting coefficient*

The cutting coefficient (CC) refers to the ratio of the rolling force and normal force [5], and the larger the CC is, the larger the torque is for the TBM cutterhead with the same thrust. The relationship between CC and h is illustrated in Figure 11. When breaking rock with static loads, the CC increases with the raise of h, and the increasing velocity slows down when h is larger than 4 mm. Under the coupled static–dynamic loads, the CC increases first and then declines with the

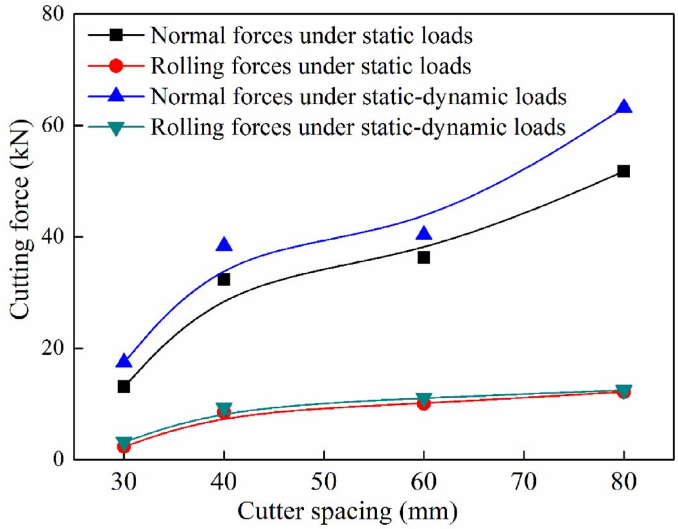

Figure 10. Relationship between cutting force and *S*.

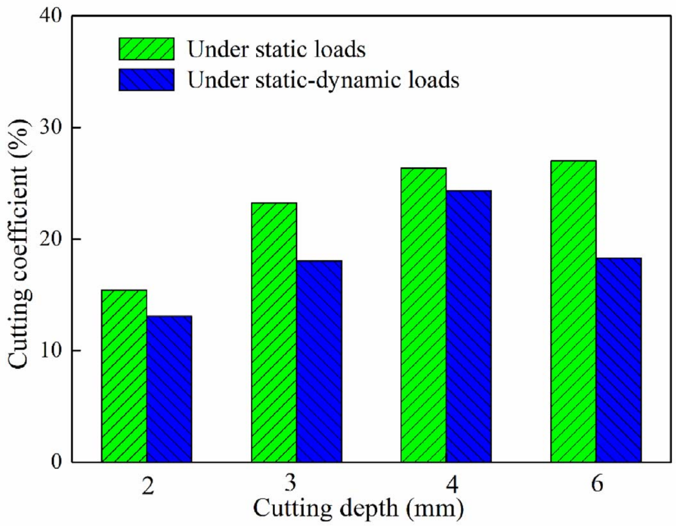

Figure 11. Relationship between CC and *h*.

increase in *h*. The changing trend of CC is consistent with that of normal and rolling forces. In addition, the CC under the coupled static–dynamic loads is smaller than that under the static loads, indicating that the torque of the cutterhead under the coupled static–dynamic loads is smaller than that under the static loads with the same thrust.

The relationship between CC and *S* is shown in Figure 12. For both cutting modes, the CC increases first and then declines with the rise in *S*. The CC reaches the peak value when *S* is 60 mm. When *S* is below 60 mm, the mutual interference within the grooves is relatively large. However, when *S* is larger than 60 mm, there is no evident interaction between the breaking grooves, leading to a decrease in CC under both types of cutting modes.

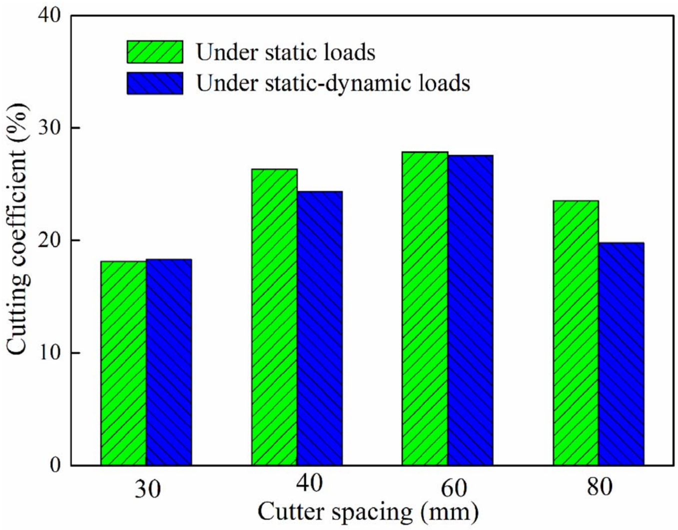

Figure 12. Relationship between CC and *S*.

3.4. *Specific energy*

The specific energy (SE) is defined as the energy required to break a unit volume of rock [27]. Generally, a large SE indicates low cutting efficiency. The value of SE can be calculated using Equation (1).

$$\mathrm{SE} = \frac{w}{v} = \frac{Fl}{v} = \frac{Fl\rho}{m} \tag{1}$$

where w is the cutting work (J), v is the breaking volume (mm^3), F is the rolling force (N), l is cutting stroke (mm), ρ is the rock density (g/mm^3), and m denotes rock broken mass (g).

The rock debris in the process of rock breaking by disc cutter is collected and weighed using an electronic balance, and three-axis force sensor records the rolling force. Then, the value of SE can be obtained using Equation (1). The relationship between SE and h is shown in Figure 13. The values of SE under the different cutting modes show a decreasing trend, and the decreasing speed gradually slows down with the increase in h. When h is smaller than 4 mm, the SE under the coupled static–dynamic loads is lower than that under the static loads. It indicates that the rock breaking efficiency of the disc cutter under the coupled static–dynamic loads is approximately 1.5 times higher than that under the static load based on the SE. When h is larger than 4 mm, the difference in the SEs for the two breaking modes becomes small. It shows that, when S is certain and h increases to a certain extent, the cutting method with coupled static–dynamic loads cannot increase the cutting efficiency anymore.

The relationship between SE and S is shown in Figure 14. The values of SE under different cutting modes show the same trend: a decreases in the first phase and then an increases with the enlargement in S. It indicates that there exists an optimal S to obtain the highest breaking efficiency and minimum SE, and the optimal S under the coupled static–dynamic loads is larger than that under the static loads, which are approximately 65 mm and 60 mm, respectively, as shown in Figure 14. For the same S, the SE under the coupled static–dynamic loads is smaller than that under the static loads on the whole. When S reaches 80 mm, the difference in the SE under the two kinds of cutting modes is the biggest. That is, when the S is relatively large, the cutting method under the coupled static–dynamic loads can improve the rock breaking efficiency significantly.

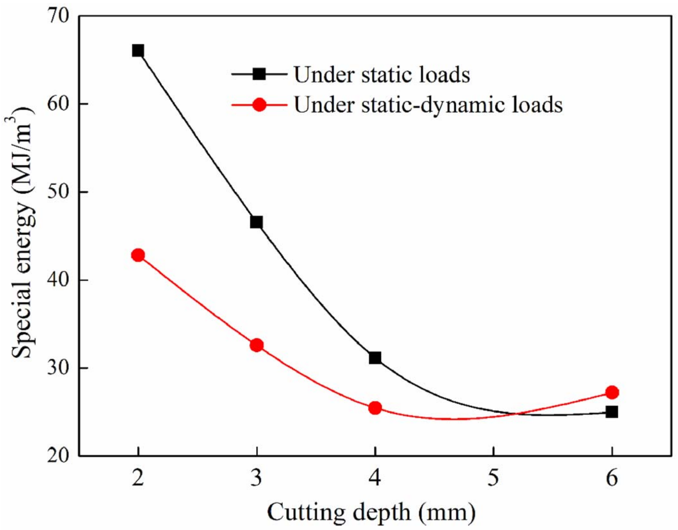

Figure 13. Relationship between SE and *h*.

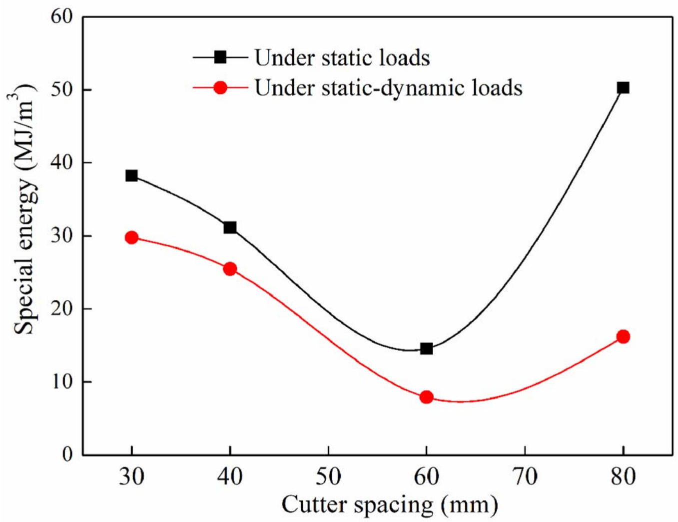

Figure 14. Relationship between SE and *S*.

4. Discussion

In recent years, TBMs have encountered some challenges in high-compressive-strength rock grounds. Considering a Chinese diversion project as an example, the highest uniaxial compressive strength of the rock from this project exceeds 300 MPa, and the cutting depth h of disc cutters is smaller than 4 mm with static loads, leading to a low rock breaking efficiency. Thus, this study aims to reveal the influence law of disc cutter breaking rock performance with impact load in extremely hard rock environments by experiments to address this issue. According to the above investigation, when the h of the disc cutter is below 4 mm, the cutting method under the coupled static–dynamic loads can significantly improve the cutting efficiency. In addition, Tan [28] established a numerical model of combined dynamic and static loading by PFC and came to a similar conclusion to this study. When the peak value and the impact frequency increase, the penetration of the disc cutter will increase, and the crack length will increase and tend to extend horizontally. The rock-crushing volume will increase, and the energy consumption of the rock-breaking ratio will decrease. Thus, when encountering hard rock grounds, the cutting method under the coupled static–dynamic loads mentioned in this paper may provide new insights for improving tunneling efficiency. Additionally, a larger optimal *S* indicates that TBM manufacturers can lay out fewer cutters on the cutterhead, i.e., when applying the coupled static–dynamic loads method, the same cutting effect can be achieved with fewer cutters and less cost compared with those under static loads.

Notably, the load and vibration on the disc cutters will be definitely enhanced and they may affect the service lives of disc cutters when cutting rock under coupled static–dynamic loads. Thus, reducing the vibration and improving the impact resistance of disc cutters are important issues to be solved when the coupled static–dynamic loads method is adopted. This paper focuses on the different rock breaking characteristics under the two methods with various of cutting depths and spacings. However, some other factors may also affect the cutter rock breaking characteristics, such as the dynamic and static loading parameters, the layout of the cutters, the type of rock, and the structural parameters of the disc cutter, which will be considered in the future work.

5. Conclusions

In this study, the rock breaking characteristics of disc cutter with different kinds of cutting modes are compared. The following conclusions are drawn:

Cutting rock under coupled static–dynamic loads is more conducive to crack propagation and formation of bigger rock debris. The average fragment size produced under the coupled static–dynamic loads is 1.6 times larger than that produced under static loads. For the two cutting methods, the average fragment size increases with the increase in h, and increases initially and then declines with the increase in cutter spacing. The largest average fragment size is obtained while S is 60 mm, which is 11.75 mm and 18.91 mm, respectively, for static and coupled static–dynamic loads.

For the two kinds of cutting modes, the normal force of the disc cutter is greater than the rolling force. When h is lower than 4 mm, the cutting force under coupled static–dynamic loads is larger than that under static loads. When h is beyond 4 mm, the cutting forces under coupled static–dynamic loads are smaller than those under static loads. Furthermore, the cutting forces for the two kinds of cutting modes increase significantly with increase in S.

The changing trend of the CC of the disc cutter is consistent with that of the cutting force, and the CC under the coupled static–dynamic loads is smaller than that under the static loads. The SE of the disc cutter decreases with the increase in h for the two cutting modes. When h is below 4 mm, the SE under the coupled static–dynamic loads is lower than that under the static loads, and the cutting method with the coupled static–dynamic loads can significantly improve the cutting efficiency. There is an optimal S that yields highest rock breaking efficiency of the disc cutter under the two cutting methods. The optimal S under the coupled static–dynamic loads is larger than that under the static loads.

As this paper describes the first time that the rock breaking tests of TBM disc cutter under coupled static–dynamic loads have been performed, more trials need to be conducted. More types of rocks need to be studied, and the optimum static–dynamic combination parameters of disc cutters for specific types of rock should be investigated in future work.

Conflicts of interest

Authors have no conflict of interest to declare.

Acknowledgements

This study was supported by the National Natural Science Foundation of China (No. 51905550), the Major Science and Technology Projects of Hunan Province (No. 2019GK1010) and the Project of State Key Laboratory of High Performance Complex Manufacturing, Central South University (No. ZZYJKT2021-15).

References

[1] L. K. Lin, Y. M. Xia, Z. G. Li, C. Z. Wu, Y. L. Cheng, Q. Tan, "Dynamic characteristics analysis with multi-directional coupling in a TBM mainframe", *Chin. J. Mech. Eng.* **32** (2019), article no. 98.

[2] S. H. Tang, X. P. Zhang, Q. S. Liu, P. Chen, X. T. Sun, L. Sun, Y. Dai, S. T. Chen, "Prediction and analysis of replaceable scraper wear of slurry shield TBM in dense sandy ground: A case study of Sutong GIL Yangtze River Crossing Cable Tunnel", *Tunn. Undergr. Sp. Tech.* **95** (2020), article no. 103090.

[3] L. K. Lin, Y. M. Xia, Q. S. Mao, X. H. Zhang, "Experimental study on wear behaviors of TBM disc cutter ring in hard rock conditions", *Tribol. Trans.* **61** (2018), p. 920-929.

[4] J. Rostami, "Study of pressure distribution within the crushed zone in the contact area between rock and disc cutters", *Int. J. Rock Mech. Min. Sci.* **57** (2013), p. 172-186.

[5] R. Gertsch, L. Gertsch, J. Rostami, "Disc cutting tests in Colorado Red Granite: Implications for TBM performance prediction", *Int. J. Rock Mech. Min. Sci.* **44** (2007), p. 238-246.

[6] M. Cardu, G. Iabichino, P. Oreste, A. Rispoli, "Experimental and analytical studies of the parameters influencing the action of TBM disc tools in tunnelling", *Acta Geotech.* **12** (2017), p. 293-304.

[7] J. Liu, P. Cao, D. Han, "Sequential indentation tests to investigate the influence of confining stress on rock breakage by tunnel boring machine cutter in a biaxial state", *Rock Mech. Rock Eng.* **49** (2016), p. 1479-1495.

[8] J. Liu, J. Wang, W. Wan, Y. Zhao, "The coupled influence of surface and internal crack propagation on rock breakages by indentations in biaxial states", *Arab. J. Sci. Eng.* **43** (2018), p. 5067-5077.

[9] Q. B. Lin, P. Cao, R. H. Cao, "Experimental investigation of jointed rock breaking under a disc cutter with different confining stresses", *C. R. Méc.* **346** (2018), no. 9, p. 833-843.

[10] Q. Geng, Z. Y. Wei, H. Meng, "An experimental research on the rock cutting process of the gage cutters for rock tunnel boring machine (TBM)", *Tunn. Undergr. Sp. Tech.* **52** (2016), p. 182-191.

[11] J. W. Cho, S. Jeon, S. H. Yu, S. H. Chang, "Optimum spacing of TBM disc cutters: A numerical simulation using the three-dimensional dynamic fracturing method", *Tunn. Undergr. Sp. Tech.* **25** (2010), p. 230-244.

[12] J. W. Cho, S. Jeon, H. Y. Jeong, S. H. Chang, "Evaluation of cutting efficiency during TBM disc cutter excavation within a Korean granitic rock using linear-cutting-machine testing and photogrammetric measurement", *Tunn. Undergr. Sp. Tech.* **35** (2013), p. 37-54.

[13] C. Labra, J. Rojek, E. Onate, "Discrete/finite element modelling of rock cutting with a TBM disc cutter", *Rock Mech. Rock Eng.* **50** (2017), p. 621-638.

[14] H. Bejari, J. K. Hamidi, "Simultaneous effects of joint spacing and orientation on TBM cutting efficiency in jointed rock masses", *Rock Mech. Rock Eng.* **46** (2013), p. 897-907.

[15] M. Z. Naghadehi, R. Mikaeil, "Optimization of tunnel boring machine (TBM) disc cutter spacing in jointed hard rock using a distinct element numerical simulation", *Period. Polytech. Civ. Eng.* **61** (2017), p. 56-65.

[16] X. P. Zhang, P. Q. Ji, Q. S. Liu, Q. Liu, Q. Zhang, Z. H. Peng, "Physical and numerical studies of rock fragmentation subject to wedge cutter indentation in the mixed ground", *Tunn. Undergr. Sp. Tech.* **71** (2018), p. 354-365.

[17] S. F. Zhai, X. P. Zhou, J. Bi, Q. H. Qian, "Validation of GPD to model rock fragmentation by TBM cutters", *Int. J. Geomech.* **17** (2016), article no. 06016036.

[18] X. P. Zhou, S. F. Zhai, J. Bi, "Two-dimensional numerical simulation of rock fragmentation by TBM cutting tools in mixed-face ground", *Int. J. Geomech.* **18** (2018), article no. 06018004.

[19] R. Ciccu, B. Grosso, "Improvement of disc cutter performance by water jet assistance", *Rock Mech. Rock Eng.* **47** (2014), p. 733-744.

[20] S. Liu, H. Ji, D. Han, C. Guo, "Experimental investigation and application on the cutting performance of cutting head for rock cutting assisted with multi-water jets", *Int. J. Adv. Manuf. Tech.* **94** (2018), p. 2715-2728.

[21] F. Hassani, P. M. Nekoovaght, N. Gharib, "The influence of microwave irradiation on rocks for microwave-assisted underground excavation", *J. Rock Mech. Geotech. Eng.* **8** (2016), p. 1-15.

[22] Q. Geng, Z. Y. Wei, H. Meng, F. J. Macias, A. Bruland, "Free-face-assisted rock breaking method based on the multi-stage tunnel boring machine (TBM) cutterhead", *Rock Mech. Rock Eng.* **49** (2016), p. 4459-4472.

[23] X. B. Li, F. Q. Gong, M. Tao, L. J. Dong, K. Du, C. D. Ma, Z. L. Zhou, T. B. Yin, "Failure mechanism and coupled static-dynamic loading theory in deep hard rock mining: a review", *J. Rock Mech. Geotech. Eng.* **9** (2017), p. 767-782.

[24] X. B. Li, T. Zhou, D. Y. Li, Z. W. Wang, "Experimental and numerical investigations on feasibility and validity of prismatic rock specimen in SHPB", *Shock Vib.* **2016** (2016), article no. 7198980.

[25] X. B. Li, Z. L. Zhou, T. S. Lok, L. Hong, T. B. Yin, "Innovative testing technique of rock subjected to coupled static and dynamic loads", *Int. J. Rock Mech. Min. Sci.* **45** (2008), p. 739-748.

[26] J. Rostami, "Performance prediction of hard rock Tunnel Boring Machines (TBMs) in difficult ground", *Tunn. Undergr. Sp. Tech.* **57** (2016), p. 173-182.

[27] R. Teale, "The concept of specific energy in rock drilling", *Int. J. Rock Mech. Min. Sci.* **2** (1965), p. 57-73.

[28] Q. Tan, T. Lao, G. J. Zhang, X. H. Zhang, L. Yi, Y. M. Xia, "Disc cutter cutting mechanism under static loading and impact dynamic loading conditions", *J. Cent. South Univ.* **49** (2018), p. 101-108 (in Chinese).